REPORT

CATALYSIS

Physical mixing of a catalyst and a hydrophobic polymer promotes CO hydrogenation through dehydration

Wei Fang[1]†, Chengtao Wang[1,2]†, Zhiqiang Liu[3]†, Liang Wang[1]*, Lu Liu[1], Hangjie Li[2], Shaodan Xu[4], Anmin Zheng[3]*, Xuedi Qin[2], Lujie Liu[1], Feng-Shou Xiao[1,5]*

In many reactions restricted by water, selective removal of water from the reaction system is critical and usually requires a membrane reactor. We found that a simple physical mixture of hydrophobic poly(divinylbenzene) with cobalt-manganese carbide could modulate a local environment of catalysts for rapidly shipping water product in syngas conversion. We were able to shift the water-sorption equilibrium on the catalyst surface, leading to a greater proportion of free surface that in turn raised the rate of syngas conversion by nearly a factor of 2. The carbon monoxide conversion reached 63.5%, and 71.4% of the hydrocarbon products were light olefins at 250°C, outperforming poly(divinylbenzene)-free catalyst under equivalent reaction conditions. The physically mixed CoMn carbide/poly(divinylbenzene) catalyst was durable in the continuous test for 120 hours.

Selective and rapid removal of water product from a reaction system has been a highly desirable pathway toward boosting catalytic performance in reactions that are restricted by water thermodynamically and/or kinetically (1, 2). Membrane reactors designed to include water-conduction nanochannels could shift the reaction equilibrium (3), but preparation of defect-free membranes at a large scale is challenging. Chemical hydrophobilization of the catalyst surface could substantially contribute to reactions by accelerating water diffusion (4–7), but in many cases the chemical interactions might change the structure of the catalyst surface or even block the active sites by hindering access of reactant molecules.

Enabling rapid water diffusion from an unchanged catalyst surface is an attractive alternative. By promoting rapid desorption of water molecules once they are formed on the catalyst surface (2), the sorption equilibrium of water is shifted, as described by $*H_2O \rightleftharpoons * + H_2O$ (* denotes the catalyst surface sites). We phys-

[1]Key Lab of Biomass Chemical Engineering of Ministry of Education, College of Chemical and Biological Engineering, Zhejiang University, Hangzhou 310027, China. [2]Key Lab of Applied Chemistry of Zhejiang Province, Department of Chemistry, Zhejiang University, Hangzhou 310028, China. [3]National Center for Magnetic Resonance in Wuhan, State Key Laboratory of Magnetic Resonance and Atomic and Molecular Physics and Mathematics, Wuhan Institute of Physics and Mathematics, Innovation Academy for Precision Measurement Science and Technology, Chinese Academy of Sciences, Wuhan 430071, China. [4]College of Materials and Environmental Engineering, Hangzhou Dianzi University, Hangzhou 310018, China. [5]Beijing Advanced Innovation Center for Soft Matter Science and Engineering, Beijing University of Chemical Technology, Beijing 100029, China.
*Corresponding author. Email: liangwang@zju.edu.cn (L.W.); zhenganm@wipm.ac.cn (A.Z.); fsxiao@zju.edu.cn (F.-S.X.)
†These authors contributed equally to this work.

ically mixed the hydrophobic promoter with the catalyst, unlike previous chemical modifications; in the syngas conversion to olefins with a cobalt-manganese carbide (CoMnC) catalyst, we achieved an increase in light olefin productivity by a factor of up to 3.4 by mixing the catalyst with the promoter. Mechanistic studies revealed that the water molecules rapidly desorbed from the catalyst surface after they formed from CO hydrogenation, which avoided the competitive adsorption with CO reactant, a crucial step in the reaction process.

The CoMnC catalyst was prepared via co-precipitation and carbonization procedures (fig. S1) (8, 9). In the syngas conversion under the given reaction conditions (H_2/CO of 2, 1800 ml g_{CoMnC}^{-1} hour^{-1}, 0.1 MPa, 250°C), the CoMnC catalyst showed a CO conversion of 32.2%, with selectivity for light olefins ($C_2^=$ to $C_4^=$) of 60.8% (fig. S2 and table S1; the CO_2 product was excluded in calculating the selectivity). In our initial attempt, we physically mixed the CoMnC catalyst with a nonporous poly(divinylbenzene) (PDVB) (water-droplet contact angle 145°, irregular morphology, surface area <5 m^2/g; table S2). This hydrophobic polymer has a chemically inert surface (fig. S3) and good thermal stability (10). The mixed catalyst, denoted CoMnC/PDVB, had substantially improved CO conversion (63.5%) and selectivity to light olefins (71.4%) (Fig. 1) relative to the CoMnC catalyst under equivalent reaction conditions. With regard to the C_{5+} by-products over CoMnC/PDVB, the proportions of pentene and hexene were 50.3% and 26.0%, respectively (table S3); these are desired products for the production of high-performance polymers and valuable chemicals (11, 12).

In particular, the molar ratios of olefin to paraffin (o/p) in these by-products were very high. For example, the o/p ratio of C_6 molecules is 14.7, which is favorable for separation and purification of desired products (13). A higher gas hourly space velocity (GHSV) of 3600 ml g_{CoMnC}^{-1} hour^{-1} decreased the CO conversion to 15.4% on the CoMnC catalyst, but the CoMnC/PDVB still showed a remarkably high CO conversion of 50.7% (table S1). Under a GHSV of 7200 ml g_{CoMnC}^{-1} hour^{-1}, the CoMnC catalyst exhibited poor CO conversion of 5.5%, whereas the CoMnC/PDVB still showed CO conversion of 19.4%. In this case, the space-time productivity of light olefins on the CoMnC/PDVB reached as high as 7.1 mmol g_{CoMnC}^{-1} hour^{-1}, which exceeded the rate for CoMnC (2.1 mmol g_{CoMnC}^{-1} hour^{-1}, carbon basis) by a factor of 3.4 (fig. S4). In addition, a CO_2 selectivity of 46.0 to 48.5% was obtained in these cases, similar to that in general Fischer-Tropsch synthesis to olefins (8, 14) and OX-ZEO (oxide-zeolite) reaction processes for converting syngas to olefins (15, 16). Adjusting the H_2/CO ratio to 3.6 and introducing a small amount of CO_2 in the syngas feed reduced the CO_2 selectivity in the products to 23.7%, giving a one-pass yield of light olefins at 28.0% (CO_2 included in calculating the olefin yield; table S4).

We compared the performance of CoMnC/PDVB to different catalysts tested previously in syngas conversion to light olefins. The data in fig. S5 show the comparison of the selectivity-conversion results reported for various catalysts in their stable period during the reaction (table S5). The general Fischer-Tropsch synthesis to olefin processes produced olefins having a wide carbon number distribution within the range C_1–C_{20} (17, 18). The selectivity of 53.0% to light olefins, with a CO conversion of 80.0% over Fe-based catalysts, has been reported as one of the most efficient processes (14), requiring a high reaction temperature of 340°C. The OX-ZEO process (15), which combines the cascade reactions of CO hydrogenation over metal oxide and C-C coupling of methanol or ketene intermediates over zeolite, showed superior selectivity to light olefins but yielded low CO conversion (e.g., 17.0% over the ZnCrO$_x$/SAPO-34 catalyst) at even higher temperatures (400°C). Relative to these processes, the reaction over the CoMnC/PDVB catalyst proceeded at lower reaction temperatures with high selectivity to light olefins and efficiently suppressed methane formation. The CoMnC/PDVB catalyst also exhibited enhanced catalytic performance relative to the bare CoMn catalyst, which has been regarded as a superior catalyst for low-temperature syngas conversion to light olefins (8).

The catalytic performance of CoMnC/PDVB catalyst was influenced by the manner of mixing of the CoMnC and PDVB components (Fig. 2, A and B, table S6, and fig. S6). Compared with a

Fig. 1. Catalytic data in light olefin production from syngas. (**A** and **B**) CO conversion (A) and hydrocarbon distribution (B) over the CoMnC and CoMnC/PDVB catalysts. Reaction conditions: 1.0 g of CoMnC catalyst or mixture containing 1.0 g of CoMnC and 1.0 g of PDVB, H_2/CO/Ar at 64/32/4, 1800 ml g_{CoMnC}^{-1} hour^{-1}, 0.1 MPa, 250°C. The error bounds were estimated by repeating the experiment more than six times. Inset in (A): Water-droplet contact angles (CAs) of CoMnC and CoMnC/PDVB. *Reaction using a feed gas of H_2/CO/Ar/CO_2 at 68/19/3/10.
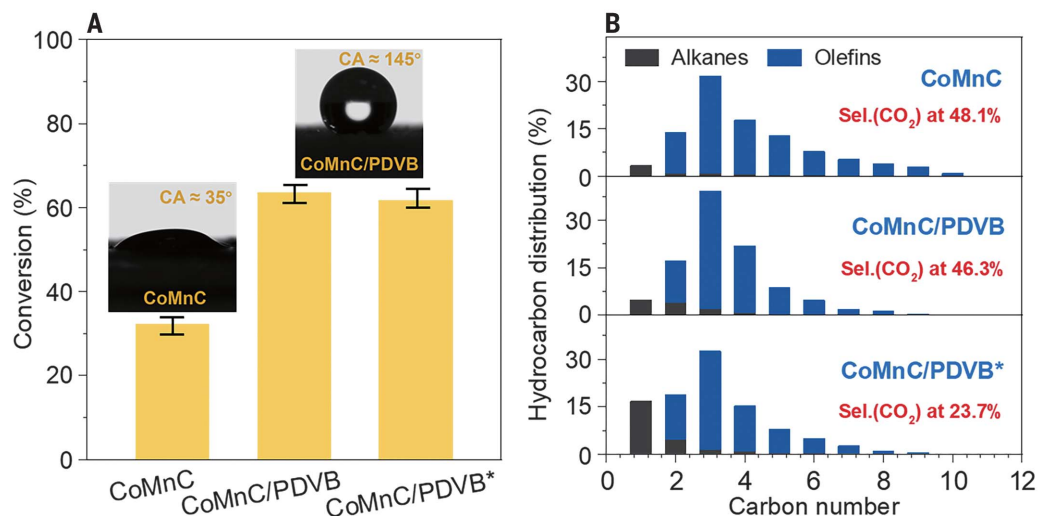
Fig. 2. Effect of different physical mixture methods and catalyst durability. (**A**) Syngas conversion performance of CoMnC/PDVB produced using different mixing techniques. Reaction conditions: 1.0 g of CoMnC and 1.0 g of PDVB, H_2/CO at 2, 1800 ml g_{CoMnC}^{-1} hour^{-1}, 0.1 MPa, 250°C. (**B**) Photographs of the catalyst beds with different mixing techniques. (**C**) Durability of CoMnC/PVDB catalyst in the syngas conversion to light olefins. Reaction conditions: 1.0 g of CoMnC catalyst physically mixed with 1.0 g of PDVB (powder-mixing), H_2/CO at 2, 1800 ml g_{CoMnC}^{-1} hour^{-1}, 0.1 MPa, 250°C.
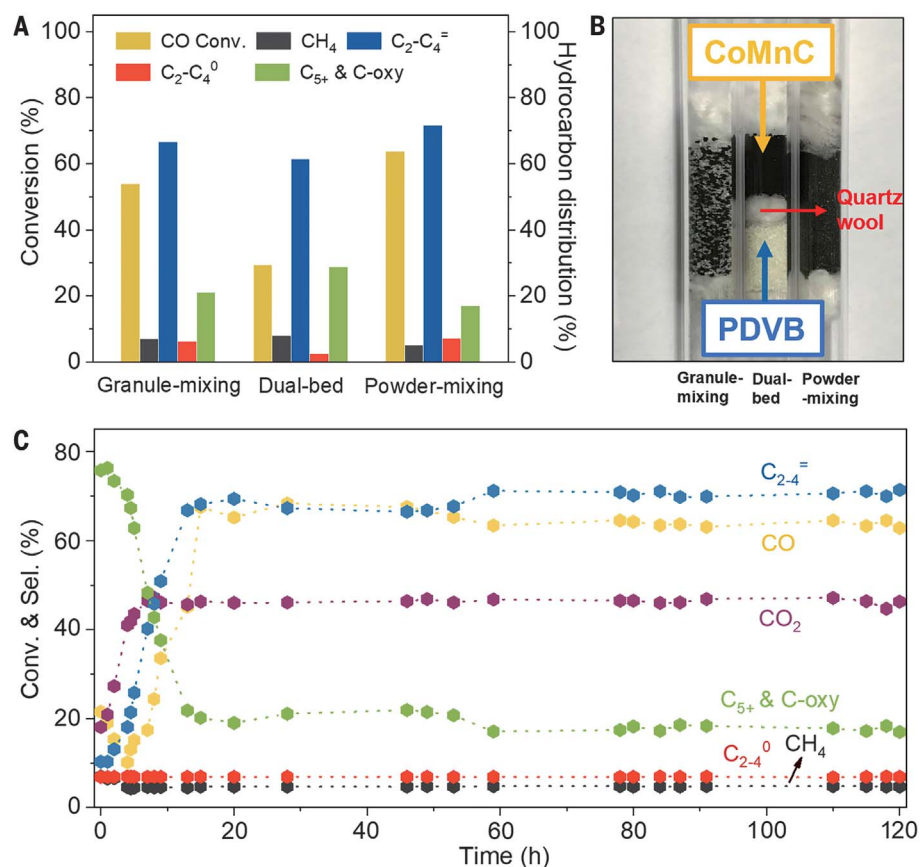
powder mixture of the CoMnC and PDVB, the granule mixture, which was prepared by granulating the CoMnC and PDVB components and then mixing them together (40 to 60 mesh), showed lower CO conversion of 53.7% and similar C_2-C_4 olefin selectivity (66.4%). In a dual-bed reactor, the PDVB was packed below the CoMnC catalyst bed and separated by a layer of inert quartz sand. The CO conversion

of 29.1% and lower olefin selectivity of 61.2% were similar to those of bare CoMnC catalyst. This result indicated that PDVB is inert for the reaction and that the promotion with PDVB required physical mixing with the CoMnC catalyst.

The CoMnC/PDVB catalyst was used in a continuous reaction test to evaluate durability. After activation for ~15 hours, the CO conver-

sion was constant at steady state with an average value of ~64.7% (Fig. 2C). Even after reaction for 120 hours, the CO conversion was well maintained at 62.8% with stable CoMnC and PDVB components, confirming the good durability of the CoMnC/PDVB. In this process, the selectivity of light olefins was also constant at 70.0%, with an average productivity at 5.9 mmol g_{CoMnC}^{-1} hour^{-1}. During the test, the

selectivities for undesired methane and C_2–C_4 alkanes remained lower than 5.0% and 7.0%, respectively. The selectivity for C_{5+} products was ~18.0%, and 92.0% of those are C_5–C_8 olefins (19, 20).

To understand the promotion of PDVB in the syngas conversion, we used temperature-programmed surface reaction mass spectrometry (TPSR-MS) by feeding syngas to the catalysts. The CoMnC catalyst has been reported to have superior activity for hydrogen activation and cleavage of the C-O bond (8, 21–23), and these steps can be identified in TPSR-MS tests. The dependences of propylene, methane, and water signals (m/z = 42, 16, and 18, respectively) on reaction temperatures (Fig. 3A) show that on the CoMnC catalyst, the water and methane signals appeared at 166° and 203°C, which we assigned to the C-O cleavage and hydrogenation reaction. At 217°C, the propylene signal began to appear because the C-C coupling step occurred after C-O dissociation. Similar signals also appeared on the CoMnC/PDVB catalysts, but the signals of propylene and water were obviously stronger

than those on the bare CoMnC, indicating that the physically mixed PDVB indeed boosted the activity.

It might be expected that the PDVB could participate in the CoMnC carbonization that leads to the distinguishable catalytic performances (22, 24). We excluded this hypothesis by characterizing the CoMnC phase change as a function of reaction time, which showed negligible difference in the x-ray diffraction (XRD) patterns of the CoMnC with and without PDVB during the reaction periods (fig. S7); this result was also supported by the TEM characterization (fig. S8). After removal of the PDVB component from the used CoMnC/PDVB catalyst, the resulting CoMnC component exhibited performance comparable to that of the as-prepared CoMnC (table S1). These results further indicate that the physical mixture with PDVB did not change the catalyst structure, and they are consistent with the high stability of PDVB at the reaction temperature (figs. S9 to S12).

The previous strategies of chemically modifying the catalyst surface with hydrophobic organosilanes were developed to improve water

resistance in syngas conversion (25–27). Following this route, we also modified the CoMn catalyst using tetraethyl orthosilicate and dimethyl diethyloxysilane, but this resulted in lower CO conversion over the CoMn@Si and CoMn@Si-c catalysts relative to the bare CoMnC catalyst (table S1). XRD patterns of the used catalysts showed the presence of oxide phases and suggested that hindered carbonization led to formation of the active CoMn carbides (fig. S13) (27).

We also varied the amount of PDVB in the catalyst bed. PDVB/CoMnC weight ratios of 0.5, 1.0, and 1.5 resulted in distinguishable CO conversions at 56.4%, 63.5%, and 70.5%, respectively (table S7). The sensitivity of CO conversion to PDVB content indicated that it plays a crucial role in catalysis. Although PDVB in the physical mixture did not change the catalyst structure, it might optimize the water diffusion because of its hydrophobicity. Thus, we studied the role of added water in CO conversion over the CoMnC catalyst (Fig. 3B). Considering that the water production rate was 8.8 to 23.5 mg g_{CoMn}^{-1} hour^{-1} in the CoMnC/PDVB-catalyzed syngas conversion (calculated according to the oxygen balance in the reaction system and the amount of collected water product after reaction; fig. S14), we added water at this rate to investigate its influence on the CO conversion. The CoMnC catalyst showed CO conversion of 33.5% at the beginning of the reaction without water injection, which then decreased to ~8.2% (average value) after water injection with a feed rate of ~10.5 mg g_{CoMn}^{-1} hour^{-1}. Interestingly, addition of PDVB to the catalyst efficiently minimized the negative effect of water, which exhibited only a relatively slight decrease in CO conversion to ~57.4% under the equivalent water feed. The activity of the CoMnC catalyst was continuously reduced as more water was added to the feed gas (fig. S15), and the CO conversion dropped to 4.7% with water feed rate of ~20.0 mg g_{CoMn}^{-1} hour^{-1}. These data confirmed the water-restricted feature of the CoMnC-catalyzed syngas conversion. In contrast, the profile of CO conversion as a function of water concentration was flatter over the CoMnC/PDVB catalyst. This hydrophobic material may have helped the water product to rapidly desorb after it was formed on the CoMnC surface and also hindered its readsorption (fig. S16), which would free up active sites for the continuous conversion of more CO molecules.

This hypothesis was supported by a pulse experiment to explore the CO adsorption on the catalyst surface with and without water injection (Fig. 3C). The CoMnC and CoMnC/PDVB catalysts were localized within the flowing He atmosphere at 250°C, with periodic pulsing of the CO or mixture of CO and water. In the test without water, the CO signals on
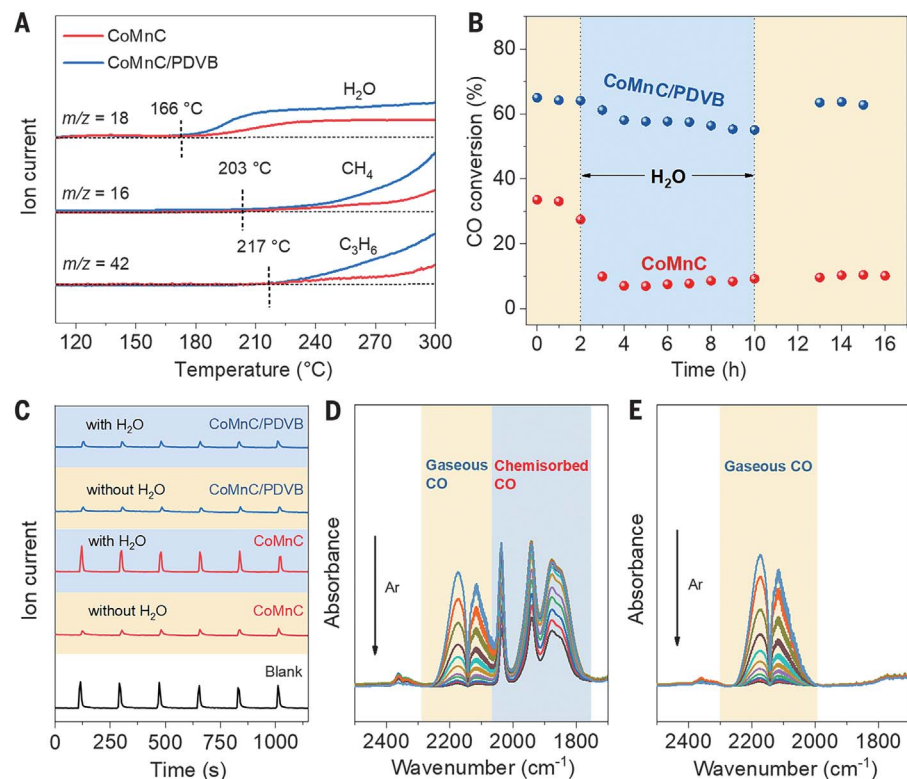

Fig. 3. PDVB-optimized water sorption. (**A**) The dependences of water, methane, and propylene signals (m/z at 18, 16, and 42) on temperature-programmed surface reaction by feeding syngas to the CoMnC and CoMnC/PDVB catalysts. (**B**) Data showing the influence of water on syngas conversion with CoMnC and CoMnC/PDVB. Reaction conditions: 1.0 g of CoMnC or 1.0 g of CoMnC physically mixed with 1.0 g of PDVB (powder-mixing), H_2/CO at 2, 1800 ml g_{CoMnC}^{-1} hour^{-1}, 0.1 MPa, 250°C. The water feed rate was ~10.5 mg g_{CoMn}^{-1} hour^{-1}. (**C**) Transient response curves obtained during pulses of 10% CO/He (5 ml/min) into pure He flow (30 ml/min) at 250°C over the CoMnC and CoMnC/PDVB catalysts. CO flowed through the water at 40°C for introducing water to the catalysts. (**D** and **E**) CO desorption in situ FTIR spectra of anhydrous CoMnC (D) and water-pretreated CoMnC catalysts (E).

both catalysts were extremely weak compared with that in the blank run without catalysts, indicating that efficient CO adsorption occurred on both CoMnC and CoMnC/PDVB catalysts. In these cases, the CO signals were similar, revealing the negligible effect of PDVB on CO sorption, and the CO adsorption dominantly occurred on the CoMnC. When water was fed into the reaction (~7 vol% in CO), the CO pulse peaks on the CoMnC catalyst were markedly increased, with the intensities similar to that in the blank run, revealing the hindered CO adsorption by competition with water.

Under the equivalent test, the CO pulse peaks were still weak on the CoMnC/PDVB catalyst, similar to the result of the water-free test, confirming the negligible influence of water on CO sorption in the presence of PDVB. A similar phenomenon was observed in the equivalent tests by changing the water feed amount (fig. S17). On the basis of these results, we conclude that the water on the catalyst surface could hinder the CO adsorption, while the PDVB efficiently shifted the sorption equilibrium described by $*H_2O \rightleftharpoons * + H_2O$ by accelerating the rapid water desorption and hindering its readsorption. These features led to a higher proportion of free catalyst surface for continuous conversion of CO, boosting the syngas conversion to olefins (fig. S18).

In situ Fourier transform infrared (FTIR) spectra characterizing the CO hydrogenation on the CoMnC and CoMnC/PDVB catalysts are shown in fig. S19. Introducing CO and hydrogen to the CoMnC catalyst led to the formation of obvious bands at 2717 to 2955 cm^{-1}, 1320 to 1527 cm^{-1}, and ~1039 cm^{-1}, which were assigned to the olefin species from CO hydrogenation and C-C coupling (28–30). The broad signals at ~1600 cm^{-1} and 3400 to 3600 cm^{-1} appeared and continuously increased with reaction time because of the water product adsorbed on the catalyst surface (31–34). On the CoMnC/PDVB catalyst, the signals of olefin products were solely observed with an extremely weak water signal, suggesting the rapid desorption of water once it is formed on the catalyst.

The effect of water on CO adsorption was further explored (Fig. 3, D and E). Introducing CO to the CoMnC catalyst led to signals of chemically adsorbed CO on the CoMnC surface (22, 33). When water was co-fed with CO, the signals of chemically adsorbed CO were almost undetectable with only the bands of gaseous CO (34), confirming that CO adsorption was hindered under competition with water. This phenomenon might explain the negative effect of water on the syngas conversion by the competitive adsorption, in good agreement with the results of pulse experiments. In contrast, the catalyst containing PDVB exhibited comparable CO adsorption with and without water injection in a FTIR
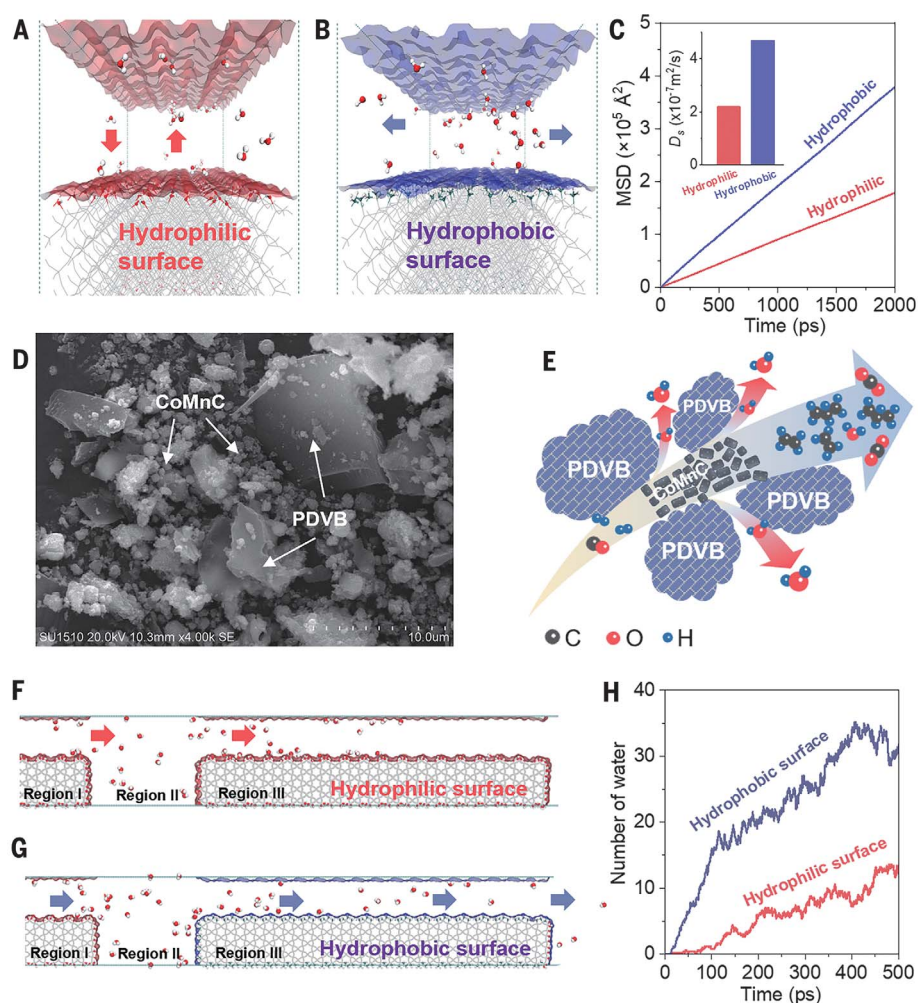
Fig. 4. Theoretical simulation. (A and B) Models showing the water diffusion within regions surrounded by hydrophilic and hydrophobic surfaces. (C) Mean square displacement (MSD) and diffusion coefficient (D_s) showing the water diffusion efficiency at 250°C. (D) SEM image of the CoMnC/PDVB granule. (E) Scheme showing the escape of water from the CoMnC surface through the region surrounded by PDVB. (F and G) Models showing the water escape through different regions. The regions I are hydrophilic and the regions III are hydrophilic and hydrophobic, respectively. (H) The number of water molecules that escaped from region III from an initial state with 100 water molecules on region I as a function of time.

study (figs. S20 and S21). According to previous studies, less water on the catalyst surface might reduce the concentration of carbon-based intermediates and enhance the hydrogenation activity (35, 36), which could explain the improved selectivity of short hydrocarbons and slightly reduced o/p ratios on the CoMnC/PDVB catalyst relative to bare CoMnC.

In addition, the olefin products adsorbing on the catalyst surface might also hinder the CO conversion to some extent, as confirmed by catalysis studies with ethylene in the syngas feed (fig. S22). However, further tests suggested a negligible effect of PDVB on olefin sorption (fig. S23). Thus, PDVB accelerated syngas conversion in the catalytic tests; this was primarily attributed to its hydrophobicity in removing water rather than olefins. We further investigated the influence of promoter wettability

on water diffusion by a theoretical simulation, in which we explored water molecule diffusion in a region surrounded by hydrophilic or hydrophobic surfaces (Fig. 4, A and B). Water diffusion efficiency was quantified by the diffusion coefficient D_s. The hydrophilic surface interacted with water molecules to slow down the transportation (Fig. 4C), giving $D_s = 2.2 \times 10^{-7}$ m^2/s. In the region surrounded by hydrophobic surfaces, the water diffusion was accelerated with obviously higher $D_s = 4.7 \times 10^{-7}$ m^2/s (Fig. 4C), given the relatively weak interaction between water and the hydrophobic surface (37). The theoretical simulation therefore gives a qualitative trend of the diffusion of water molecules along the different surface.

In our work, the CoMnC catalyst and PDVB were physically mixed and randomly distributed

in the catalyst granules. As observed in the scanning electron microscope (SEM) image of an actual CoMnC/PDVB catalyst granule (Fig. 4D), the CoMnC and PDVB were packed tightly and disordered, with intergranular distances ranging from nanometers to micrometers (Fig. 4E). We studied how the hydrophobic promoter affects the escape of water that is produced on the relatively hydrophilic surface (e.g., the CoMnC surface). In Fig. 4, F and G, we show models simulating the water escape from the solid surface (region I) through the region surrounded by hydrophobic or hydrophilic surfaces (region III), respectively. Notably, these regions were separated from each other (region II) for simulating the physical mixing with intergranular distances between the CoMnC and PDVB granules in the catalyst (figs. S24 and S25).

The number of escaped water molecules as a function of diffusion time in the systems with hydrophobic and hydrophilic promoters, from an initial state with 100 water molecules on region I (Fig. 4H), indicated that more water molecules escaped through the hydrophobic channel than from the hydrophilic channel under the equivalent conditions. For example, after 500 ps, ~32% of the initial water molecules escaped from the model with the hydrophobic channel, whereas only 13% escaped from the model with the hydrophilic channel. The influence of water concentration on diffusion rate was also simulated by regulating the number of water molecules in region I of the initial state (e.g., 25, 50, and 100 water molecules; fig. S26). The results showed that increasing the concentration of water molecules on the hydrophobic model surface could accelerate the diffusion rate of water molecules, which helps to explain the rapid water diffusion in the syngas conversion reaction with continuously produced water molecules. The models showed that the hydrophobic promoter physically regulated the catalyst by accelerating the water diffusion, in good agreement with the experimental results.

PDVB-promoted water sorption can also be directly observed through a model experiment of $CuSO_4 \cdot 5H_2O$ dehydration, because of its color change from blue to white upon dehydration. After mixing a small amount of PDVB to the $CuSO_4 \cdot 5H_2O$ (0.75 wt% of PDVB in the mixture), the color change was obviously accelerated, as confirmed by the photographs in fig. S27. This result again confirms that PDVB promoted water desorption and hindered readsorption when physically mixed.

We prepared physical mixtures of CoMnC catalyst with different materials whose wettability was distinguishable. When nanopores were introduced to the PDVB (two nanoporous PDVB materials with distinguishable surface areas at 488.2 and 623.3 m^2/g; table S2 and figs. S28 to S31), the CO conversion further improved to 88.7% and 92.4% over the CoMnC/nanoporous PDVB catalysts, but selectivity for light olefins was at 53.4% and 37.6% (table S1). Relative to CoMnC/PDVB, the CoMnC/nanoporous PDVB catalysts showed higher selectivity for the heavier olefins (C_5 to C_8 selectivity of 33.7% and 43.7%, respectively). This phenomenon might be the result of the high adsorption capacity of nanoporous PDVB for the olefin products (fig. S32), which prolonged the retention time of olefin products in the catalyst bed to benefit chain growth. These data confirmed that product distribution could be adjusted by changing the nanoporosity of the PDVB promoter.

Similar trends were also observed in the reaction with the CoMnC catalyst mixed with methyl group–modified silica with a hydrophobic surface (SiO_2-Me, figs. S33 to S35), which showed CO conversion at 74.7% and lower selectivity for C_2–C_4 olefins at 45.5% (table S1). Higher selectivity for C_5–C_8 products and lower o/p ratios were obtained than with the reaction over CoMnC/PDVB. When graphite, a hydrophobic carbon material, was mixed with CoMnC (CoMnC/Gra, fig. S36), the CO conversion was 53.0% with 67.3% selectivity for light olefins (table S1). Given that the graphite is earth-abundant and extremely cheap, our strategy for shifting water-mediated sorption equilibrium could be implemented simply by mixing hydrophobic graphite with the current catalysts.

In addition, when relatively hydrophilic materials (such as a mixture of PDVB, SiO_2, and hydrophilic polymers; figs. S37 to S40) were used in the CoMnC-catalyzed syngas conversion, the CO conversion was markedly reduced (tables S8 to S10). For example, polystyrene (PS, fig. S40), which has composition similar to PDVB but is more hydrophilic, failed to promote the CoMnC-catalyzed syngas conversion, showing CO conversion at 10.7% with methane selectivity of 37.8% and C_2–C_4 olefin selectivity of 37.8% (table S10). These data show the importance of a hydrophobic promoter.

Our approach could be used to upgrade industrially catalytic processes without modifying the catalysts themselves. In addition, the strategy is conceptually different from catalyst hydrophilization with organosilanes, described as a chemical modification route, where the conversion was not obviously improved in syngas conversion but the CO_2 selectivity was reduced by hindering the undesired water-gas shift (4). This difference might result from the distinguishable distances between the active site and the hydrophobic surface for these different systems. Considering that many hydrogenation reactions are strongly affected by water, the physical regulation method using a promoter with desired wettability could guide the design of more efficient catalysts in the future.

REFERENCES AND NOTES

1. M. Wolf, N. Fischer, M. Claeys, *Nat. Catal.* **3**, 962–965 (2020).
2. H. Li *et al.*, *Science* **367**, 667–671 (2020).
3. S. M. Hashim, A. R. Mohamed, S. Bhatia, *Rev. Chem. Eng.* **27**, 157–178 (2011).
4. Y. Xu *et al.*, *Science* **371**, 610–613 (2021).
5. S. Crossley, J. Faria, M. Shen, D. E. Resasco, *Science* **327**, 68–72 (2010).
6. H. Yang, T. Zhou, W. Zhang, *Angew. Chem. Int. Ed.* **52**, 7455–7459 (2013).
7. Z. Jin *et al.*, *Science* **367**, 193–197 (2020).
8. L. Zhong *et al.*, *Nature* **538**, 84–87 (2016).
9. R. Yang *et al.*, *J. Energy Chem.* **32**, 118–123 (2019).
10. Y. Zhang *et al.*, *Nano Today* **4**, 135–142 (2009).
11. P. Ramírez de la Piscina, J. L. G. Fierro, J. Sales, N. Homs, *Catal. Lett.* **14**, 45–49 (1992).
12. W. Fan, P. Wu, T. Tatsumi, *J. Catal.* **256**, 62–73 (2008).
13. R. Yang, R. Gao, Z. Qian, Y. Wang, *Separ. Purif. Tech.* **230**, 115884 (2020).
14. H. M. Torres Galvis *et al.*, *Science* **335**, 835–838 (2012).
15. F. Jiao *et al.*, *Science* **351**, 1065–1068 (2016).
16. K. Cheng *et al.*, *Angew. Chem. Int. Ed.* **55**, 4725–4728 (2016).
17. S. Soled, E. Iglesia, R. A. Fiato, *Catal. Lett.* **7**, 271–280 (1990).
18. M. D. Shroff *et al.*, *J. Catal.* **156**, 185–207 (1995).
19. T. Ren, M. Patel, K. Blok, *Energy* **31**, 425–451 (2006).
20. R. Snel, *Catal. Rev., Sci. Eng.* **29**, 361–445 (1987).
21. H. Wang *et al.*, *J. Am. Chem. Soc.* **135**, 4149–4158 (2013).
22. Z. Li *et al.*, *ACS Catal.* **7**, 3622–3631 (2017).
23. F. Jiang *et al.*, *Catal. Today* **369**, 158–166 (2021).
24. Y. Yang *et al.*, *Appl. Catal. A* **549**, 179–187 (2018).
25. R. Xie *et al.*, *Catal. Commun.* **12**, 589–592 (2011).
26. M. Ojeda *et al.*, *Langmuir* **22**, 3131–3137 (2006).
27. X. Yu *et al.*, *Appl. Catal. B* **232**, 420–428 (2018).
28. C. J. Weststrate, J. W. Niemantsverdriet, *ACS Catal.* **8**, 10826–10835 (2018).
29. C. J. Weststrate, I. M. Ciobîcă, J. van de Loosdrecht, J. W. Niemantsverdriet, *J. Phys. Chem. C* **120**, 29210–29224 (2016).
30. A. A. Efremov, A. A. Davydov, *React. Kinet. Catal. Lett.* **15**, 327–331 (1980).
31. L. Marchese, J. Chen, J. M. Thomas, S. Coluccia, A. Zecchina, *J. Phys. Chem.* **98**, 13350–13356 (1994).
32. K. Tanaka, J. M. White, *J. Phys. Chem.* **86**, 4708–4714 (1982).
33. D. J. C. Yates, *J. Phys. Chem.* **65**, 746–753 (1961).
34. C.-J. Jia *et al.*, *J. Am. Chem. Soc.* **133**, 11279–11288 (2011).
35. A. K. Dalai, B. H. Davis, *Appl. Catal. A* **348**, 1–15 (2008).
36. C. J. Bertole, C. A. Mims, G. Kiss, *J. Catal.* **210**, 84–96 (2002).
37. K. Liu, X. Yao, L. Jiang, *Chem. Soc. Rev.* **39**, 3240–3255 (2010).

Science

Physical mixing of a catalyst and a hydrophobic polymer promotes CO hydrogenation through dehydration

Wei FangChengtao WangZhiqiang LiuLiang WangLu LiuHangjie LiShaodan XuAnmin ZhengXuedi QinLujie LiuFeng-Shou Xiao

Channeling water away

Heterogeneous catalytic reactions that produce water as a by-product can be inhibited by its presence on the surface. Fang *et al.* found that for the production of light olefins from syngas (a 2:1 mixture of hydrogen and carbon monoxide) with a cobalt manganese carbide catalyst at 250°C, the addition of the hydrophobic polymer polydivinylbenzene as part of a physical mixture almost doubled the conversion of carbon monoxide (see the Perspective by Ding and Xu). Theoretical models suggest that the polymer formed channels that accelerated water diffusion away from the catalyst. —PDS

View the article online
https://www.science.org/doi/10.1126/science.abo0356
Permissions
https://www.science.org/help/reprints-and-permissions

Use of this article is subject to the Terms of service